

Asymmetric space-dependent systems through stochastic noise: Partial stabilization and exact solutions for a class of nonlinear Langevin equations

Kwok Sau Fa * ^{†,1}, Choon-Lin Ho,² Y. B. Matos,¹ and M. G. E. da Luz ^{‡1}

¹*Departamento de Física, Universidade Federal do Paraná, 81531-980 Curitiba-PR, Brazil*

²*Department of Physics, Tamkang University, Tamsui 25137, Taiwan*

Abstract

In many instances, the dynamical richness and complexity observed in natural phenomena can be related to stochastic drives influencing their temporal evolution. For example, random noise allied to spatial asymmetries may induce stabilization of otherwise diverging trajectories in a nonlinear dynamics. However, how exactly this type of phenomenology takes place in actual processes is usually very difficult to identify. Here we unveil few trends leading to dynamical stabilization and diversity by introducing Gaussian noise to a class of exactly solvable non-linear deterministic models displaying space-dependent drifts. For the resulting nonlinear Langevin equations, the associated Fokker-Planck equations can be solved through the similarity method or the Fourier transform technique. By comparing the cases with and without noise, we discuss the changes in the system's dynamical behavior. Simple cases of drift and diffusion coefficients are explicitly analyzed and comparisons with some other models in the literature are made. Our study illustrates the behavioral richness originated from spatially heterogeneous dynamical systems under the influence of white noise.

PACS numbers: 05.40.-a, 05.40.Ca, 02.50.Ey

Keywords: Nonlinear Langevin equation; dynamical stabilization and diversity; Fokker-Planck equation; multiplicative white noise; anomalous diffusion

* Permanent address: Department of Physics, Universidade Estadual de Maringá, Av. Colombo 5790, 87020-900, Maringá-PR, Brazil

[†] corresponding author email: kwok@dfi.uem.br

[‡] email: luz@fisica.ufpr.br

I. INTRODUCTION

The diversity of responses to external stimuli is one of the key factors generating the behavioral richness common to many natural phenomena [1, 2]. For instance, this can give rise to the emergence of complexity and spatial-temporal patterns in a broad range of processes [3, 4], even if they are restricted to certain constraints (say, having to follow a gradient flow) as in the evolution of coarsening systems [5, 6].

There are distinct features allowing for such variety of evolution trends (for a review see, e.g., [7]). But certainly, spatial heterogeneities and/or asymmetries are among the most ubiquitous ones [8–11]. Indeed, effects like spatial-temporal oscillations [12], resonances [13] and strong dispersion [14] can all be triggered by inhomogeneous environments. This is particularly true in biologically-related problems where space-dependent coefficients may greatly influence the variability of population genetics [15–17] and growth [18–25], the type of diffusion across membranes [26], and the onset of anomalous mobility [27], just to cite a few situations. It is also needless to emphasize that landscape profile changes are fundamental to understand large and strongly correlated systems, as in ecology [4, 9, 10].

Nonetheless, as relevant as to induce distinct comportment, spatially asymmetric interactions and drives have a crucial role in stabilizing, synchronizing and promoting cooperative feedback [28–32], essential to maintain the functional diversity in the natural world [33–37] by preventing trivial dynamics [7]. On the other hand, the existence of a phase or state space displaying multi-stability [38, 39] — conceivably created by heterogeneous media — is not enough to avoid falling into trivial attractors [40]. Thence, escaping or switching mechanisms from dynamical traps [41, 42] are commonly found in systems displaying rich features in time evolution, notably in non-equilibrium as well as in complex systems [43]. Given that randomness is very effective in leading to such mechanisms [44, 45], the somewhat omnipresence of stochasticity in our (diverse) physical world is far from being a surprise [1, 2, 36, 45].

The above discussion supports the well known significance of the generalized Langevin equation (GLE) in describing countless realistic processes, appealing rather directly to our intuition — for an overview see [46] as well the refs. therein. It combines the deterministic Newton’s second law with drift to external stochastic forces [47–52]. However, the GLE is a stochastic differential equation, and so is generally difficult to treat for arbitrary drifts

and random forces. One possible approach is to convert the GLE into the deterministic Fokker-Planck equation for the associated probability density function (PDF). Then, one can exploit the large number of methods available in the literature for solving differential equations. This constitutes a traditional framework to tackle countless problems, particularly those whose important physical quantities depend non-trivially on space. As examples we mention the modeling of: transport processes [53, 54], organic semiconductors [55], periodic porous material [56], and turbulent two-particle diffusion in configuration space [57–61]. Further, in the case of drifts with time-dependent coefficients (even if implicitly), the Fokker-Planck approach helps to understand unusual dynamics, as the asymptotic of continuous time random walk models [62], logarithmic oscillations for moments of physical variables [63] and dynamical diversity for systems driven by colored noise [64–71].

In the present contribution we shall address the interplay between deterministic and stochastic dynamics. We discuss a way to avoid steady (trivial) and monotonic diverging behavior by adding noise to a spatially asymmetric dynamical evolution, partially stabilizing the system [38]. To keep the problem as simple as possible — but yet displaying spatial heterogeneity — we suppose a set of one-dimensional systems whose drift coefficients depend on the sign of their dependent variable $x(t)$. For such prototype models we first show that the pure deterministic evolution tends to be rather undiversified in a very large region of the parameters space. Then, we include a generic multiplicative noise driven by the Gaussian white noise in the Stratonovich prescription. This yields nonlinear Langevin equations, displaying anomalous diffusion. Following a previously developed method [72] and a transformation scheme amenable to systems possessing scaling similarity [52, 73–77], we are able to exactly solve the corresponding Fokker-Planck equation for a considerably large range of parameter values. For some cases where this prescription does not work, we use the Fourier transform technique. From the analytic solutions we analyze the difference between the evolution with and without the stochastic component. In particular, we examine how the stochasticity evades dynamical steady behavior and also how the emerging evolution diversity depends on the specific regions of the system parameters space.

Finally, concrete simple examples are explored in more details. The resulting PDFs are studied for some parameter values and few cases are compared with related traditional models in the literature.

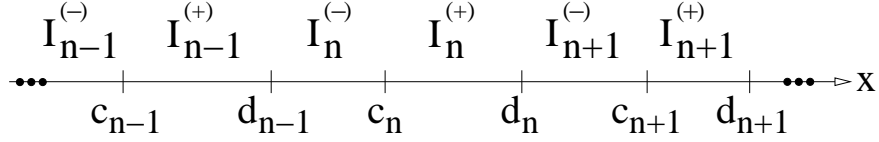


FIG. 1: Schematics of the successive distinct intervals along x for which the function $G(x)$, basically the integral of $D(x)$, changes its sign.

II. THE SET OF MODELS

A. Deterministic dynamical system

Consider a one-dimensional dynamical variable $x(t)$, whose evolution is governed by the equation

$$\frac{dx(t)}{dt} = \left(a - b \mu \frac{\text{sign}(G(x))}{2} \right) |G(x)|^{\mu-1} D(x), \quad (1)$$

with initial condition $x(t_0) = x_0$. Here, a , b and μ are real numbers with $b > 0$, $\text{sign}[\cdot]$ is the sign function, $D(x)$ is a given everywhere non-negative function of x , and $G(x)$ relates to $D(x)$ through

$$\frac{dG(x)}{dx} = \frac{1}{D(x)}. \quad (2)$$

Different $D(x)$'s specify distinct drift terms and so we have in fact a set of systems.

Although $D(x) \geq 0$, $G(x)$ may assume positive or negative values depending on x . Thus, along the infinite line x we can identify the intervals $c_n < x < d_n$ as $I_n^{(+)}$ and $d_{n-1} < x < c_n$ as $I_n^{(-)}$ (see Fig. 1), such that in $I_n^{(+)}$ ($I_n^{(-)}$) the function $G(x) > 0$ ($G(x) < 0$). By supposing $G(x)$ a continuous function, for any integer $n \in (N_l, N_r)$, inevitably $G(c_n) = G(d_n) = 0$. This is not the case if we allow “jumps” for $G(x)$ whenever x crosses over between positive and negative intervals $I^{(+)}$ and $I^{(-)}$. If for all $x > x_r$ ($x < x_l$), $\text{sign}[G(x)]$ does not change, then N_r (N_l) is a finite integer, otherwise $N_r \rightarrow \infty$ ($N_l \rightarrow -\infty$).

By noticing that $|G(x)|^{\mu-1} D(x)$ is never negative, in principle the term $\text{sign}[G(x)]$ in Eq. (1) should give rise to a non-trivial spatially asymmetric evolution depending on the parameter values. To see why, let us consider that during the time interval $\mathcal{I}_T : t_0 \leq t < T$, the r-h-s of Eq. (1) does not vanish. Hence

- (i) For $|a|/b > |\mu|/2$ the time derivative of x has always the same signal of a . As a consequence, $x(t)$ presents a steady increasing ($a > 0$) or decreasing ($a < 0$) behavior for $t \in \mathcal{I}_T$ regardless of the functional form of $G(x)$.

- (ii) On the other hand, for $|\mu|/2 > |a|/b$, it follows that $dx(t)/dt$ has the same sign of $-\mu G(x)$. Therefore, along the evolution of $x(t)$ in the time interval \mathcal{I}_T , we have a switching in the variation of $x(t)$ whenever $G(x(t))$ reverses its sign, conceivably originating a rich dynamics depending on $D(x)$.

However, the system ceases to evolve when the r-h-s of Eq. (1) becomes zero. This always takes place if along the time evolution of $x(t)$ there is a $x(\bar{t}) = \bar{x}$ such that either $a/b - \text{sign}[G(\bar{x})]\mu/2 = 0$ (in which case $|a|/b = |\mu|/2$) or

$$|G(\bar{x})|^{\mu-1}D(\bar{x}) = 0. \quad (3)$$

Disregarding the too specific and trivial situation of $|a|/b = |\mu|/2$, for an oscillatory-like dynamics described in (ii) to occur (say, within the interval (x_{min}, x_{max})), Eq. (3) must be precluded. For so, we observe that if $D(\bar{x}) = 0$ ($|G(\bar{x})|^{\mu-1} = 0$) then $|G(\bar{x})|^{\mu-1} (D(\bar{x}))$ must diverge in such way to maintain their product non-null as $x \rightarrow \bar{x}$. Therefore, suppose that in the vicinity of \bar{x} the leading term from either a Taylor or a Laurent series for $D(x)$ and $G(x)$ is (for both $\nu, \gamma \neq 0$)

$$D(x) \approx d(x - \bar{x})^\nu, \quad G(x) \approx g(x - \bar{x})^\gamma, \quad (4)$$

with the constants $d, g \neq 0$. So, we should have

$$\nu + (\mu - 1)\gamma \leq 0 \quad \Rightarrow \quad \nu \leq (1 - \mu)\gamma. \quad (5)$$

Moreover, from Eqs. (2) and (4) it follows that $gd\gamma \approx 1$ and $\gamma + \nu \approx 1$, thus

$$(2 - \mu)\nu \leq 1 - \mu. \quad (6)$$

We remark that Eq. (6) fails when $\mu = 2$.

Particular cases are easily derived from the above. Let us assume \bar{x} in the interval of interest (x_{min}, x_{max}) , then Eq. (3) is not verified at $x = \bar{x}$ in the following situations:

- (a) If $\mu = 1$, when $D(\bar{x}) \neq 0$. Thence, in the full x interval we must have $D(x) > 0$.
- (b) For $D(\bar{x}) = 0$ (so $\nu > 0$) then: (b-1) if $\mu < 1$, when $\nu \leq (1 - \mu)/(2 - \mu) < 1$ (so that $G(\bar{x}) = 0$); (b-2) if $\mu > 2$, when $\nu \geq (\mu - 1)/(\mu - 2) > 1$ (such that $G(\bar{x})$ diverges).

- (c) For $\mu > 1$ and $G(\bar{x}) = 0$, when $1 < \mu < 2$. In fact, here we must have a diverging $D(\bar{x})$, implying in $\nu < 0$. This condition requires the mentioned range for μ .
- (d) If there are jumps in $D(x)$, so that $G(x)$ can change signal but without passing through zero, then when $D(x) > 0$. However, in such case we should define a proper prescription for Eq. (2) at these discontinuities.

It is clear from the above analysis that only for specifically chosen functions $D(x)$ and parameter values, namely, those observing the restrictions (a)–(d), the asymmetric term in Eq. (1) can yield a more diverse, eventually stable or recurrent, dynamics. This is in opposition to a simple, as sink or diverging, basins of attraction emerging for Eq. (1) for generic $D(x)$'s, i.e., functions not complying with (a)–(d).

To illustrate the previous discussion, we give three examples of $D(x)$ and the associated $G(x)$ in Fig. 2, assuming the parameters in the range specified by (ii). In Fig. 2 (a) we have functions with proper jumps to observe the condition (d). In this case $|G(x)|^{\mu-1} D(x)$ is never null, but at the expense of rather specially tailored discontinuous $D(x)$ and $G(x)$. In Fig. 2 (b), $D(x) = \sin^2[x]$ and $G(x) = -\cot[x]$, with $\mu = 3$. At the zeros of $D(x)$, one finds that $G(x)^2 D(x) > 0$ — hence precluding Eq. (3) — since the condition (b) is verified (note that $G(x)$ diverges at these points). Nevertheless, at the zeros of $G(x)$ we cannot avoid $G(x)^2 D(x)$ also to vanish, so with Eq. (3) holding true. Consequently, the system dynamics necessarily halts at these sink points. Lastly, for $D(x) = 1/2 + \sin^2[x]$, $G(x) = 2 \arctan[\sqrt{3} \tan[x]]/\sqrt{3}$ and $\mu = 11/10$, we have that $|G(x)|^{0.1} D(x)$ is never null. But this demands very narrow divergences for $|G(x)|^{0.1} D(x)$ (observe the spikes in the Fig. 2 (c)), hence also for $dx(t)/dt$, whenever x is very close to multiples of π . This type of drift might be unacceptable in modeling distinct processes.

In this way, a natural question is what would stabilize our family of dynamical systems, averting a trivial evolution from Eq. (1) — where by trivial we mean $x(t)$ either becoming stationary or monotonically evolving towards $\pm\infty$ — for a much broader set of functions $D(x)$ and parameter values. We shall demonstrate below this can be achieved via stochastic noise added to the original deterministic problem.

For completeness, the formal general solution of the present dynamical system in each interval $I^{(\pm)}$ is presented in the Appendix A.

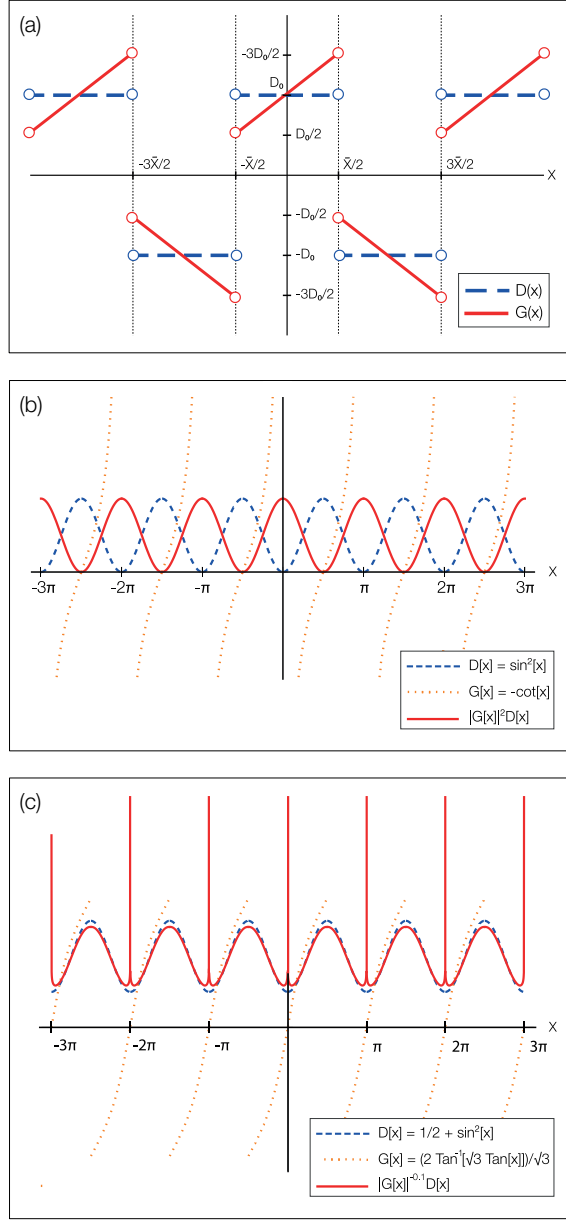


FIG. 2: Three examples of $D(x)$ and $G(x)$. In (a) and (c), the term $|G(x)|^{\mu-1} D(x)$ is never zero, potentially resulting in a rich dynamics for $x(t)$. But this requires very particular and singular functions. In (b) although $|G(x)|^{\mu-1} D(x)$ does not vanish in the points where $D(x) = 0$, this cannot be avoided for the points where $G(x) = 0$, eventually driving the system to a stationary behavior.

B. Adding stochastic noise

Hereafter we consider an extra noise term in our original model. In doing so, we obtain a nonlinear Langevin equation — in the Stratonovich description — with space-dependent drift and diffusion coefficients, and driven by a Gaussian white noise, reading

$$\frac{dx(t)}{dt} = \left(a - b\mu \frac{\text{sign}(G(x))}{2} \right) |G(x)|^{\mu-1} D(x) + \sqrt{b} |G(x)|^{\mu/2} D(x) L(t). \quad (7)$$

The parameter values ranges and relation between $D(x)$ and $G(x)$ are as before. The white noise force, $L(t)$, is such that [47]

$$\langle L(t) \rangle = 0, \quad \langle L(t)L(t') \rangle = 2\delta(t-t'). \quad (8)$$

Now we should emphasize that the previous situation of dynamical traps for the deterministic model, represented by Eq. (3), is far less common here. Indeed, provided $a \pm b\mu/2 \neq 0$ and $\mu \neq 2$ in Eq. (7), for a given $x(t) = \bar{x}$ to lead to $dx(t)/dt = 0$ (so stationary) independently on the noise $L(t)$, it should at once satisfy Eq. (3) as well as an akin relation with $\mu - 1 \rightarrow \mu/2$ (for the second term in the r-h-s of Eq. (7)). But based on our previous analysis, this simultaneous condition is very unlikely to happen for an arbitrary function $D(x)$. Furthermore, for some very specific possible values of $L(t)$, instantly the sum of the two terms in r-h-s of Eq. (7) could become zero. However, this exact cancelation would cease at subsequent times as $L(t)$ varies.

The corresponding Fokker-Planck equation for the Langevin equation (7) in the Stratonovich approach is given by [47]

$$\frac{\partial \rho(x, t)}{\partial t} = -\frac{\partial}{\partial x} \left[\left(a |G(x)|^{\mu-1} + b |G(x)|^\mu \frac{dD(x)}{dx} \right) D(x) \rho(x, t) \right] + b \frac{\partial^2}{\partial x^2} [|G(x)|^\mu D^2(x) \rho(x, t)], \quad (9)$$

where $\rho(x, t)$ is the probability distribution function (PDF).

III. EXACT SOLUTIONS AND ANALYSES OF EQ. (9)

In this section we shall address our model family given by Eq. (9). In doing so, we need to consider two distinct situations, $\mu \neq 2$ and $\mu = 2$. Exact solutions are then derived by means of proper variable transformations and by using, respectively, the similarity method for the former and the Fourier transform method for the latter. More concrete and detailed examples are discussed in Sec. IV.

A. The case $\mu \neq 2$: Solutions from the similarity method

Equation (9) can be cast as

$$\frac{\partial \rho(x, t)}{\partial t} = -a \frac{\partial}{\partial x} \left[|G(x)|^{\mu-1} D(x) \rho(x, t) \right] + b \frac{\partial}{\partial x} \left[D(x) \frac{\partial}{\partial x} (|G(x)|^\mu D(x) \rho(x, t)) \right]. \quad (10)$$

Thus, from the transformations

$$\bar{x} = G(x), \quad \bar{\rho}(\bar{x}, t) = D(x) \rho(x, t), \quad (11)$$

we obtain the following Fokker-Planck equation:

$$\frac{\partial \bar{\rho}(\bar{x}, t)}{\partial t} = -a \frac{\partial}{\partial \bar{x}} \left[|\bar{x}|^{\mu-1} \bar{\rho}(\bar{x}, t) \right] + b \frac{\partial^2}{\partial \bar{x}^2} \left[|\bar{x}|^\mu \bar{\rho}(\bar{x}, t) \right]. \quad (12)$$

The above is invariant under the rescaling (with γ arbitrary)

$$\bar{x} \rightarrow \epsilon \bar{x}, \quad t \rightarrow \epsilon^{2-\mu} t, \quad \bar{\rho} \rightarrow \epsilon^\gamma \bar{\rho}. \quad (13)$$

Thus, we can employ the similarity solution method [52, 74, 75] to address Eq. (12).

For $\bar{\rho}(\bar{x}, t) = t^{-\alpha} \Phi(z)$ and $z = \bar{x}/t^\alpha$, with the scaling exponent $\alpha = 1/(2 - \mu)$, Eq. (12) reduces to the ordinary differential equation (for \mathcal{A} a constant)

$$b \frac{d}{dz} \left(|z|^\mu \Phi \right) + \left(\alpha z - a |z|^{\mu-1} \right) \Phi = \mathcal{A}. \quad (14)$$

By setting $\mathcal{A} = 0$ in Eq. (14) (for our purposes here we do not need to address the $\mathcal{A} \neq 0$ case), it readily follows that

$$\Phi(z) = C \frac{|z|^{\frac{a}{b} \text{sign}(z) - \mu}}{b} \exp \left[-\frac{|z|^{2-\mu}}{b(2-\mu)^2} \right], \quad (15)$$

where C represents the normalization constant. Therefore, a solution for Eq. (9) in the case of $\mu \neq 2$ reads

$$\rho(x, t) = C \frac{|G(x)|^{\frac{a}{b} \text{sign}(G(x)) - \mu}}{b D(x) t^{\frac{1-\mu + \frac{a}{b} \text{sign}(G(x))}{2-\mu}}} \exp \left[-\frac{|G(x)|^{2-\mu}}{b(2-\mu)^2 t} \right]. \quad (16)$$

Note that the spatial asymmetry is manifested in Eq. (16) through the term $\text{sign}[G(x)]$. For a vanishing a , such asymmetry disappears. We highlight that the PDF in Eq. (16) can display a broad range of behaviors depending on $D(x)$ and the corresponding $G(x)$.

The normalization condition for $\rho(x, t)$ is the same than that for $\Phi(z)$, so that we should have

$$\int_{-\infty}^{\infty} \rho(x, t) dx = \int_{-\infty}^{\infty} \Phi(z) dz = 1, \quad (17)$$

since $G(\pm\infty) \rightarrow \pm\infty$. From Eq. (17) we obtain the following normalization constant by formal integration

$$C = \frac{(b(2-\mu)^2)^{\frac{1}{2-\mu}}}{|2-\mu| \left((b(2-\mu)^2)^{-\frac{a}{b(2-\mu)}} \Gamma \left[\frac{1-\mu-\frac{a}{b}}{2-\mu} \right] + (b(2-\mu)^2)^{\frac{a}{b(2-\mu)}} \Gamma \left[\frac{1-\mu+\frac{a}{b}}{2-\mu} \right] \right)}, \quad (18)$$

where $\Gamma[\cdot]$ denotes the Gamma function. We find that the PDF (16) is not normalizable for $1 \leq \mu < 2$ (actually, the similarity method is not the most appropriate method to treat the $\mu = 2$ case, see next section). Similarly, one of the following two restrictions must also be verified for a proper C :

- If $\mu < 1$, then $\mu < 1 - |a|/b$,
- If $\mu > 2$, then $\mu > 1 + |a|/b$.

Usually, for an arbitrary $D(x)$ the computation of the n -moment, given by $\langle x^n(t) \rangle$, is not an easy task. On the other hand, the generalized n -moment $\langle G^n(x) \rangle$ is far more amenable to calculations. In order to obtain the generalized n -moment we take the whole space $(-\infty, \infty)$ for x , supposing a generic $D(x) \geq 0$ (but we notice that special cases might be simpler to handle, for instance, $G(x) = x$ if $D(x) = 1$ then we recover the ordinary n -moment $\langle x^n(t) \rangle = \langle G^n(x(t)) \rangle$). As an extra condition, we assume $G(\pm\infty) \rightarrow \pm\infty$. In this way, from $\int_{-\infty}^{\infty} G^n(x) \rho(x, t) dx$ we have

$$\langle G^n(x) \rangle = C |2-\mu| (b(2-\mu)^2)^{\frac{n-1-\frac{a}{b}}{2-\mu}} t^{\frac{n}{2-\mu}} \times \left((-1)^n \Gamma \left[\frac{n+1-\mu-\frac{a}{b}}{2-\mu} \right] + (b(2-\mu)^2)^{\frac{2\frac{a}{b}}{2-\mu}} \Gamma \left[\frac{n+1-\mu+\frac{a}{b}}{2-\mu} \right] \right). \quad (19)$$

Repeating the same type of analysis for Eq. (19) as previously, we find that the generalized n -moment is finite only if

- $\mu < 2$: $n+1 > \mu + |a|/b$,
- $\mu > 2$: $n+1 < \mu - |a|/b$.

B. The case $\mu = 2$

For the particular case of $\mu = 2$ we employ variable transformations and Fourier transform method. Now we rewrite Eq. (9) as follows.

$$\frac{\partial \rho(x, t)}{\partial t} = -\frac{\partial}{\partial x} \left[(a - b \operatorname{sign}(G(x))) H(x) \rho(x, t) \right] + b \frac{\partial}{\partial x} \left[H(x) \frac{\partial}{\partial x} (H(x) \rho(x, t)) \right], \quad (20)$$

where $H(x) = |G(x)| D(x)$. For simplicity, we restrict ourselves to the case where $\text{sign}(G(x))$ assumes a unique value. Considering

$$\frac{dx^*}{dx} = \frac{1}{H(x)} \quad \text{and} \quad \rho^*(x, t) = H(x) \rho(x, t), \quad (21)$$

we obtain the following Fokker-Planck equation

$$\frac{\partial \rho^*(x^*, t)}{\partial t} = -\frac{\partial}{\partial x^*} [(a - b \text{sign}(G(x))) \rho^*(x^*, t)] + b \frac{\partial^2}{\partial x^{*2}} \rho^*(x^*, t). \quad (22)$$

Its solution is obtained from the Fourier transform method supposing the initial condition $\rho^*(x^*, 0) = \delta(x^* - x_0^*)$. The final result is then [72]

$$\rho(x, t) = \frac{C}{\sqrt{4\pi b t} H(x)} \exp \left[-\frac{(x^*(x) - x_0^* - (a - b \text{sign}(G(x))) t)^2}{4 b t} \right], \quad (23)$$

for C the correct normalization constant.

We should remark that the PDF in Eq. (23) is also the solution for the case of zero drift, but for the position coordinate x^* translated by

$$x^*(x) \rightarrow x^*(x) - (a - b \text{sign}(G(x))) t. \quad (24)$$

C. The qualitative dynamical evolution of the deterministic and stochastic models in the parameters space

So far we have discussed the deterministic and stochastic models, analyzing their features and solutions in terms of ranges of values for the associated parameters. In particular, we have unveiled that in most instances, the non-linear deterministic model of Eq. (1) tends to display rather straightforward trends. In fact, it would require specific conditions (both for the set $\{a, b, \mu\}$ as well for the properties of $D(x)$ and the corresponding $G(x)$) so to yield a rich dynamics for $x(t)$, say oscillating between two extrema, x_{min} and x_{man} , instead of approaching a fixed point \bar{x} in finite time or asymptotically evolving towards $\pm\infty$.

Conversely, by adding white noise to our original problem, we have obtained a non-linear Langevin equation, given by Eq. (7). In this case dynamical traps are far more rare and the evolution of the now stochastic $x(t)$ is not affected by most of the restrictions discussed in Sec. II A for the deterministic case. Rather than to investigate in detail such stochastic microscopic variable, we have followed the standard procedure of considering the related

probability density function $\rho(x, t)$, seeking for general non-trivial solutions displaying spatial asymmetry. For instance, note that relevant changes of behavior for ρ do take place depending on the term $\text{sign}(G(x))$ appearing in Eq. (16) (explicit examples in the next section).

Thus, keeping in mind the obvious conceptual differences between the physical meaning of $x(t)$ governed by Eq. (1) and $\rho(x, t)$ by Eq. (10), we could contrast the ranges for the set $\{a, b, \mu\}$, which in one hand may result in a rather simple monotonic dynamics for the deterministic problem, but on the other hand might allow phenomenologically much more diverse behavior for the stochastic model (cf., Eq. (16)). This kind of comparison can be viewed as a heuristic or even operational way of inferring how stochasticity can lead to the emergence of complexity in certain classes of systems [78, 79].

In this way, we need to address only the instances where $x(t)$ in Eq. (1) can asymptotically diverge since the scarcity of dynamical traps for Eq. (7) has already been discussed (see the paragraph following Eq. (8) in Sec. II B). We restrict the analysis to $\mu \neq 2$. Hence, for our purposes we rewrite Eq. (7) as

$$\frac{dx(t)}{dt} = \mathcal{F}(x) \left(\mathcal{G}(x) + L(t)/\sqrt{b} \right), \quad (25)$$

where $\mathcal{F}(x) = b|G(x)|^{\mu/2} D(x) \geq 0$ and $\mathcal{G}(x) = (a/b - (\mu/2) \text{sign}(G(x))) |G(x)|^{\mu/2-1}$. We also recall the condition (i) in Sec. II A, namely,

$$|a|/b > |\mu|/2. \quad (26)$$

For it, regardless of $G(x)$ the dynamical evolution of the deterministic model (in the absence of traps) is monotonic, i.e., $x(t)$ always increases or decreases with t .

Further, we should emphasize the known fact [80] that for a non-linear Langevin equation, determined characteristics of the resulting non-linear trajectories — noticeably divergence [81, 82] — may hinder a proper PDF ensemble description via a linear Fokker-Planck equation (for a comprehensive discussion see, e.g., [83]). For example, it poses important issues related to stability and solvability of the latter [82, 84].

In Sec. III we present the parameter intervals for which the stochastic model is or is not solvable. It is not if $1 \leq \mu < 2$, when from Eq. (25) combined with Eq. (26) it follows that $\mathcal{G}(x)$ is either always positive (+) or always negative (−), moreover with $-1/2 \leq \mu/2 - 1 < 0$ and $b < 2|a|/|\mu|$. So, in the long run the fluctuations from $L(t)/\sqrt{b}$ cannot change the

evolution tendency of $x(t)$ towards $\pm\infty$, determined by $\mathcal{G}(x)$. Notice that very qualitatively $x(t)$ resembles a kind of random walk, but with a spatial bias in a determined direction. Hence, it leads to a divergence for the related $\rho(x, t)$ — as mentioned above, a kind of ensemble of these non-linear (and here diverging) paths. In other words, in this case the stochastic noise cannot stabilize the system.

When $\mu > 2$ (and $|a|/b > 1$), from Eq. (26) the deterministic model is monotonic for $2 < \mu < 2|a|/b$, tending to $\pm\infty$ if there are no dynamical traps along the way. But for $\mu > 2$, the stochastic model is well behaved provided $\mu > 1 + |a|/b$ (Sec. III). Thence, stabilization of the dynamical system can also be attained in the extra interval $1 + |a|/b < \mu \leq 2|a|/b$ through the addition of white noise. Nonetheless, in the remaining range $2 < \mu < 1 + |a|/b$ in which Eq. (1) diverges, again for the stochastic model the function $\mathcal{G}(x)$ in Eq. (25) has always a same sign. Consequently, the above argument used for $1 \leq \mu < 2$ likewise applies.

Lastly, for $\mu < 1$ the dynamical model is monotonic in the interval $-2|a|/b < \mu < \min(1, 2|a|/b)$. On the other hand, the stochastic model is solvable and normalizable when $\mu < 1 - |a|/b$. Accordingly, the white noise is not able to stabilize the system only for $1 - |a|/b < \mu < \min(2|a|/b, 1)$. Given that such parameters range corresponds to $\mathcal{G}(x)$ never inverting its sign, the previous reasoning once more explains this result.

IV. SOME SPECIFIC EXAMPLES FOR THE STOCHASTIC MODEL

Next we illustrate by means of simple, but representative, examples some trends of the PDF ρ 's presented in Sec. III. In Sec. IV A we consider $\mu \neq 2$ and $D(x) = 1$. This is an interesting choice because in this case the generalized n -moment reduces to the standard $\langle x^n \rangle$'s. In Sec. IV B we address $\mu = 2$. In particular, for a specific $D(x)$ we show that our system relates to important population growth models in the literature.

A. The case of $\mu \neq 2$ and $D(x) = 1$

For $D(x) = 1$ we have $G(x) = x + \text{constant}$. For simplicity we set such constant to zero. We just comment that depending on a , b and μ (and the initial condition x_0), the dynamical system can either become stationary or diverging.

In Eq. (7), $|G(x)|^{\mu-1} = |x|^{\mu-1}$ and $|G(x)|^{\mu/2} = |x|^{\mu/2}$ give rise to distinct power-law

functions. The normalized PDF reads (for C in Eq. (18))

$$\rho(x, t) = C \frac{|x|^{\frac{a}{b} \text{sign}(x) - \mu}}{b t^{\frac{1 - \mu + \frac{a}{b} \text{sign}(x)}{2 - \mu}}} \exp \left[-\frac{|x|^{2 - \mu}}{b(2 - \mu)^2 t} \right]. \quad (27)$$

It is interesting to note that the PDF described by Eq. (27), for $\mu = a/b$ and $\mu < 1$, is composed of a stretched or compressed Gaussian distribution and a generalized Weibull distribution. This dual functional form suggests that the system described by Eq. (7) may be used to describe processes resulting from different dynamical drives.

The n -moment can be obtained from Eq. (19), yielding

$$\begin{aligned} \langle x^n \rangle &= C |2 - \mu| (b(2 - \mu)^2)^{\frac{n-1-\frac{a}{b}}{2-\mu}} \\ &\times \left((-1)^n \Gamma \left[\frac{n+1-\mu-\frac{a}{b}}{2-\mu} \right] + (b(2 - \mu)^2)^{\frac{2\frac{a}{b}}{2-\mu}} \Gamma \left[\frac{n+1-\mu+\frac{a}{b}}{2-\mu} \right] \right) t^{\frac{n}{2-\mu}}. \end{aligned} \quad (28)$$

In the particular case of $a = 0$, the PDF in Eq. (27) reduces to

$$\rho(x, t) = \frac{(b(2 - \mu)^2)^{\frac{1}{2-\mu}} |x|^{-\mu}}{2b|2 - \mu| \Gamma \left[\frac{1-\mu}{2-\mu} \right] t^{\frac{1-\mu}{2-\mu}}} \exp \left[-\frac{|x|^{2-\mu}}{b(2 - \mu)^2 t} \right], \quad (29)$$

and Eq. (28) results in (with $C_0 = C|_{a=0}$)

$$\langle x^n \rangle = C_0 |2 - \mu| (b(2 - \mu)^2)^{\frac{n-1}{2-\mu}} \Gamma \left[\frac{n+1-\mu}{2-\mu} \right] ((-1)^n + 1) t^{\frac{n}{2-\mu}}. \quad (30)$$

One can see that $\langle x^n \rangle$ in Eq. (30) is zero for n an odd number, in accordance with the symmetric PDF in Eq. (29). In particular, its second moment goes with $t^{2/(2-\mu)}$, hence it can describe, superdiffusive, normal and subdiffusive, processes respectively for, $0 < \mu < 1$, $\mu = 0$ and $\mu < 0$. Further, for $\mu > 2$ the system describes localized processes.

Generally, the PDF in Eq. (27) represents a system with a power-law potential of order higher than 2 when $\mu > 2$ and with a spatial asymmetry associated with the term $a \text{sign}(x)$, or (with $a \neq 0$ and $b\mu/2 - a \text{sign}(x) > 0$)

$$V(x) \sim \frac{(b\mu/2 - a \text{sign}(x))}{\mu} |x|^\mu. \quad (31)$$

Thus, the parameter $|a|$ determines the degree of asymmetry, with $a = 0$ leading to a totally symmetric PDF, Eq. (29).

The solution given by Eq. (27) is not valid for $\mu = 2$. Nonetheless, we can take $\mu \sim 2$, so that $|G(x)|^{\mu-1}$ (related to the non-linear drift and with the asymmetry term $\text{sign}(G(x))$) and $|G(x)|^{\mu/2}$ (related to the white noise coefficient) in Eq. (7) are both approximately linear in

$|G(x)|$. In this case the $V(x)$ in Eq. (31) with $\mu \sim 2$ fairly represents the usual symmetric (asymmetric) harmonic potential for $a = 0$ ($a \neq 0$ and $b/2 > |a|$).

We can also compare the PDF in Eq. (29) with that one obtained from Eq. (7), but without drift and derived in different prescriptions, or (see the ref. [52])

$$\rho(x, t) = \frac{|x|^{-(1-\lambda)\mu}}{2|2-\mu|^{\frac{-(1-2\lambda)\mu}{2-\mu}} \Gamma\left[\frac{1-(1-\lambda)\mu}{2-\mu}\right] (bt)^{\frac{1-(1-\lambda)\mu}{2-\mu}}} \exp\left[-\frac{|x|^{2-\mu}}{b(2-\mu)^2 t}\right]. \quad (32)$$

Here $0 \leq \lambda \leq 1$ is the prescription parameter, for $\lambda = 1/2$ yielding the Stratonovich's and $\lambda = 0$ the Ito's. The n -moment for to the PDF in Eq. (32) is

$$\langle x^n(x) \rangle = \frac{(b(2-\mu)^2)^{\frac{n}{2-\mu}} \Gamma\left[\frac{n+1-(1-\lambda)\mu}{2-\mu}\right] t^{\frac{n}{2-\mu}}}{\Gamma\left[\frac{1-(1-\lambda)\mu}{2-\mu}\right]}, \quad (33)$$

where n is an even number. Observe that Eq. (32) coincides with Eq. (29) for $\lambda = 0$ (the Ito prescription). This follows directly from the fact that for the Fokker-Planck equation in Eq. (9), the drift term vanishes since for $D(x) = 1$ we have $dD(x)/dx = 0$. Moreover, the n -moment in Eq. (33) has similar behavior of that in Eq. (30) for even numbers.

All these findings show that there are a large class of systems displaying the same n -moment trends.

Finally, graphs of Eq. (27) for distinct parameter values (all with $a > 0$) and at different time instants t are depicted in Figs. 3–6. For $a \rightarrow -a$ we get a specular image, about $x = 0$, of the observed profiles. Since $G(x) = x$, which is anti-symmetric in x , all the plots display an imbalance regarding positive and negative x 's, hence overall with $\rho(x < 0)$ much greater than $\rho(x > 0)$. Also, the imbalance tends to be stronger for greater $|a|$'s. For Figs. 3–5 (6 (a) and 6 (b)) we have $\xi = \mu - 1 > 0$ ($\xi = 1 - \mu > 0$), so that $|G(x)|^{\mu-1} D(x) = |x|^\xi$ ($|G(x)|^{\mu-1} D(x) = 1/|x|^\xi$). This explains why the corresponding PDFs are very small (very large) for x approaching zero. From the plots for $\mu > 2$ we see that as t increases, the distributions tend to concentrate around the origin. We have checked this is likewise the case for the examples with $\mu < 1$ (not shown), but then with such concentration taking place slower in time. As a last remark, provided a and b are the same and the values of the associated μ 's do not differ much, for the examples here we have not detected relevant qualitatively differences between the ρ 's either when $2a/b < \mu < 1 - a/b$ or when $\mu < 2a/b < 1 - a/b$ if $\mu < 1$ and when $\mu > 1 + a/b > 2a/b$ or when $2a/b > \mu > 1 + a/b$ if $\mu > 2$.

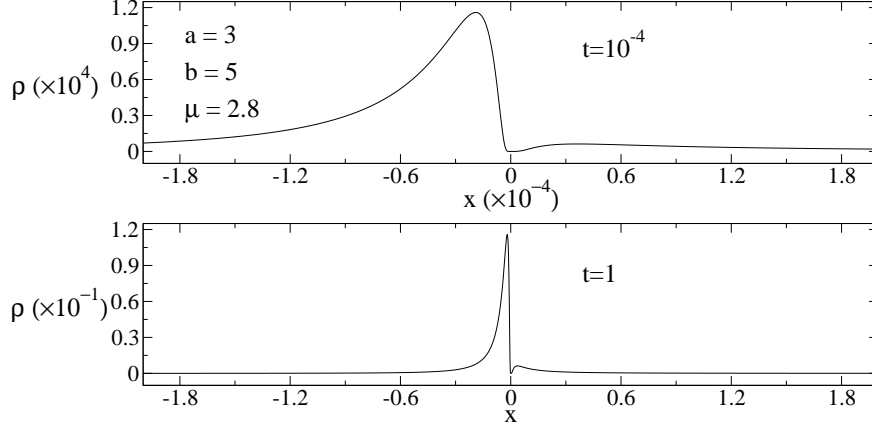


FIG. 3: For the case of $D(x) = 1$, the resulting PDF, Eq. (27), at two time instants, $t = 1$ and the very short $t = 10^{-4}$ (on purpose, to illustrate the shape of the initial PDF). For the parameters a , b and μ considered, $\mu > 2 > 1 + a/b > 2a/b$, thus not belonging to the monotonic behavior (i) for the dynamical system. Although the distribution is considerably higher for $x < 0$, it is still noticeable for x positive, but only in the origin vicinity. In the plots, both ρ and x have been rescaled so to facilitate a direct comparison between the curves shapes. Notice that ρ is spatially much more concentrated at $t = 1$ than at $t = 10^{-4}$.

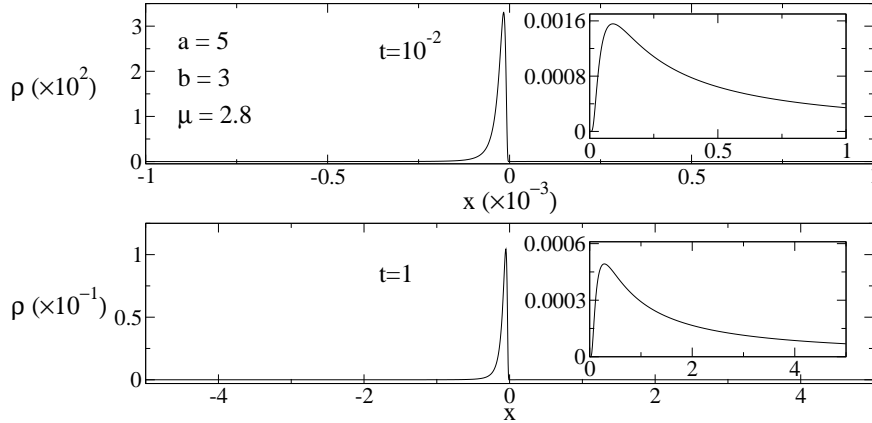


FIG. 4: Similar plots as in Fig. 3, but for the parameters values such that $2a/b > \mu > 1 + a/b > 2$. Hence, the corresponding dynamical system does belong to the monotonic behavior class (i). Since now the PDFs are very small for x positive, the insets show proper blow ups for $x > 0$. Again, ρ is spatially much more concentrated at $t = 1$ than at $t = 10^{-2}$.

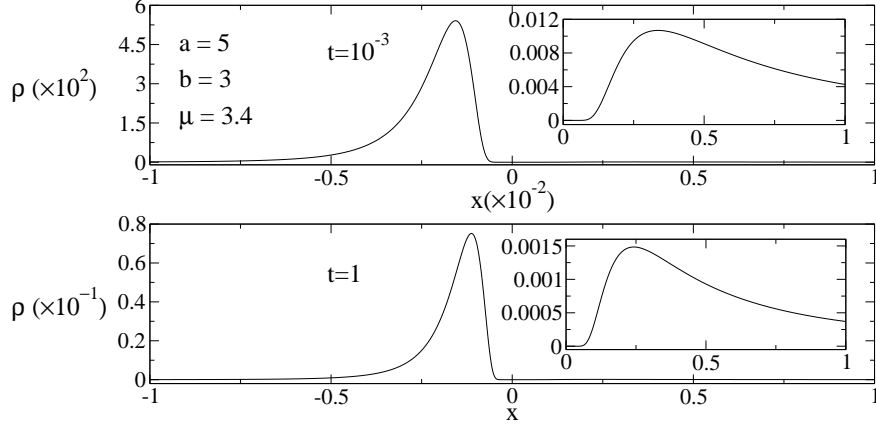


FIG. 5: Similar plots as in Fig. 4, but for the parameters satisfying $\mu > 2a/b > 1 + a/b > 2$. Thus, as in Fig. 3, not belonging to the monotonic behavior (i) for the dynamical system. The PDF is spatially much more concentrated at $t = 1$ than at $t = 10^{-3}$.

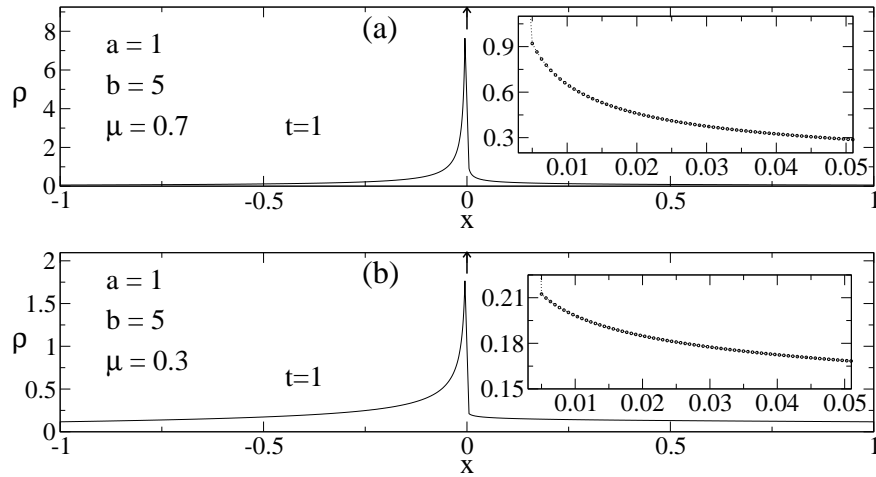


FIG. 6: For $D(x) = 1$, the PDF in Eq. (27) at $t = 1$ with $a = 1$, $b = 5$ and two values of $\mu < 1$. (a) $\mu = 0.7$, thus $2a/b < \mu < 1 - a/b < 1$. (b) $\mu = 0.3$, thus $\mu < 2a/b < 1 - a/b < 1$. The arrows indicate that although integrable, these ρ 's tend to $+\infty$ at the origin. The insets give details of the distributions for $x > 0$ very close to the origin. These PDF's tend to be more concentrate as t increases, plots not shown.

B. Some examples for $\mu = 2$

We finally consider the solution in Eq. (23). For $H(x) = \sqrt{h}$, with h a positive constant, we have $x^*(x) = x/\sqrt{h}$, $|G(x)| = \exp[\pm x/\sqrt{h}]$ and $D(x) = \sqrt{h} \exp[\mp x/\sqrt{h}]$. In this case, the PDF in Eq. (23) recovers the well-known ρ for a Brownian motion with a load force,

whose expression is [71]

$$\rho(x, t) = \frac{1}{\sqrt{4\pi b h t}} \exp \left[-\frac{(x - x_0 - \sqrt{h}(a - b)t)^2}{4 b h t} \right]. \quad (34)$$

A particularly interesting situation — relating to other models in the literature — results from $H(x)$ given by

$$H(x) = \frac{(K^\alpha - x^\alpha) x}{\beta K^\alpha - (\beta - \alpha) x^\alpha}, \quad (35)$$

such that

$$D(x) = \frac{K^\beta}{K^\alpha} \frac{(K^\alpha - x^\alpha)^2 x^{1-\beta}}{(\beta K^\alpha - (\beta - \alpha) x^\alpha)}, \quad G(x) = \frac{(x/K)^\beta}{1 - (x/K)^\alpha}. \quad (36)$$

In this case, the PDF in Eq. (23) is related to the population growth model proposed in [22] (see also [20]). More specifically, $0 \leq x(t) \leq K$ is the number of alive individuals in a population at time t , $r = a - b \operatorname{sign}(G(x)) = a - b$ is the intrinsic growth rate with $a > b$, and K is the carrying capacity. For simplicity, the parameters β and α are restricted to real non-negative values. In fact, the system described by Eqs. (7) and (35) encompasses classical growth models such as the Verhulst logistic ($\beta = 1$ and $\alpha = 1$), Gompertz ($\beta = 0$ and $\alpha \rightarrow 0$), Shoener ($\beta = 0$ and $\alpha = 1$), Richards ($\beta = 0$ and $0 < \alpha < \infty$) and Smith ($0 \leq \beta < \infty$ and $\alpha = 1$) [18–25]. Also, for $\beta = \alpha = 1$ the present framework has been employed in the study of population genetics [15].

In formulating the above mentioned models through the present approach, some care is necessary concerning the normalization constant. For instance, to avoid a time dependent C (implying in a non-conservation of probability along t), the limits of integration for ρ , $x_i^*(x = 0)$ and $x_f^*(x = K)$, should not be finite. This is determined from (recall that $dx^*/dx = 1/H(x)$)

$$x^* = \ln \left[\frac{(x/K)^\beta}{1 - (x/K)^\alpha} \right]. \quad (37)$$

As an example we consider the Shoener and Richards models (both with $\beta = 0$). They cannot be constructed under the present procedure once the lower limits have finite values. Indeed, for $\beta = 0$ and $\alpha > 0$ we get $x^* = -\ln[1 - (x/K)^\alpha]$, so that x_i^* is zero for $x = 0$.

For $\beta, \alpha \neq 0$ we have $x^*(x \rightarrow 0) \rightarrow -\infty$ and $x^*(x \rightarrow K) \rightarrow \infty$. Thus, from Eq. (23) we find $C = 1$ and the PDF yields (with $t_0 = 0$)

$$\rho(x, t) = \frac{1}{\sqrt{4\pi b t H(x)}} \exp \left[-\frac{(x^*(x) - x_0^* - (a - b)t)^2}{4 b t} \right]. \quad (38)$$

In general x_0^* is considered finite (except for $\alpha \rightarrow 0$). Thus, one should exclude a population that is initially null ($x_0 \rightarrow 0$) or that is already at its maximum possible value established by K ($x_0 \rightarrow K$)

V. CONCLUSION

In this contribution we have considered a set of models with asymmetric space-dependent drifts. For the deterministic case, we have identified their temporal evolution features in the parameters space $\Lambda = \{a, b, \mu\}$ and also in terms of certain general properties of the driven function $D(x)$ (and of its primitive integral $G(x)$). We have shown the deterministic models display rather simple behavior in a large region of Λ .

Then, by adding Gaussian noise to such class of problems we have obtained nonlinear Langevin equations, whose associated Fokker-Planck equations have been solved through the similarity method or Fourier transform method. In the subset of Λ where the obtained ρ 's are well behaved, we have discussed the dynamical richness emerging from these PDFs. For instance, conceivably they could be used to study anomalous diffusion, with applications in different processes as population growth models.

By comparing the two families of models in Λ , we have unveiled the effects of introducing stochasticity and the mechanisms allowing the qualitative changes observed in the systems dynamics. Concretely, we have found that for some regions of Λ , although the trajectories of the deterministic models are trivial, i.e., either fall into fixed points or evolve to $\pm\infty$, in the stochastic case they become stable. By stable we mean the orbits are more complex, however no longer diverging or going into sinks.

In conclusion, to understand how the natural laws, so economical in number and so simple in structure, determine the huge behavioral richness perceived in the physical world is one of the great challenges in science [1–4, 7]. It has been long known that random inputs [44, 45], in otherwise deterministic systems, can account for part of such multiplicity [28–32]. Although much progress has been achieved, the effects promoting diversity in noise-assisted dynamical evolution are very far from a complete description (see, for instance, [40–43]). We hope that at least for particular instances, the present theoretical results can help to shed some light into this crucial query.

Acknowledgments

We would like to thank G. V. Viswanathan for a critical reading of earlier versions of the present manuscript and M. W. Beims for helpful discussions about stabilization processes in dynamical systems. MGEL acknowledges financial support from CAPES (via the CAPES PRINT-UFPR program “Efficiency in uptake, production and distribution of photovoltaic energy distribution as well as other renewable sources of renewable energy sources”) Grant No. 88881.311780/2018-00 and CNPq for the research Grant No. 304532/2019-3. YBM acknowledges CAPES for a PhD scholarship.

Appendix A: The implicit analytic solution for the dynamical system represented by Eqs. (1) and (2)

Our dynamical system can be solved analytically by considering the successive spatial intervals $I_n^{(\pm)} = (c_n^{(\pm)}, d_n^{(\pm)})$ — with $\text{sign}[G(x \in I_n^{(\pm)})] = \pm 1$ — to which $x_n(t)$ belongs to at the corresponding time intervals \mathcal{I}_n . The full trajectory $x(t)$ is then given by the proper concatenation of these piecewise $x_n(t)$ for $t \in \mathcal{I}_n$.

So, here we discuss only the functional form of $x(t)$ in an arbitrary $I^{(+)}$ or $I^{(-)}$ with $t \in \mathcal{I} = (t_0, T)$ and for simplicity assuming the starting point $x_0 = x(t_0)$ in the interior of $I^{(\pm)}$. We observe that in concrete instances, one also should correctly deal with the behavior of $x(t)$ in crossing from a spatial interval $I^{(\pm)}$ to $I^{(\mp)}$. But as seen in Sec. II A, this demands to know the exact form of $D(x)$.

For the following let us set $G_0 = G(x_0)$ and denote by \tilde{G} the formal inverse function of G . Hence, for all x it holds that $\tilde{G}(G(x)) = x$.

1. $x(t) \in I^{(+)}$ for the time interval $t \in (t_0, T)$

In this case $G(x) \geq 0$ (with the equality only at the borders of $I^{(+)}$) and

$$\frac{dx(t)}{dt} = c G(x)^{\mu-1} D(x), \quad (\text{A1})$$

with $c = a - b\mu/2 \neq 0$ (of course, $c = 0$ leads to a trivial solution). Note that $G_0 > 0$.

Then, by the direct integration of Eq. (A1) taking into account Eq. (2), we find that

$(t \in (t_0, T))$

$$\begin{aligned} x(t) &= \tilde{G}([c(2-\mu)(t-t_0) + G_0^{2-\mu}]^{1/(2-\mu)}), & \text{for } \mu \neq 2, \\ x(t) &= \tilde{G}(G_0 \exp[c(t-t_0)]), & \text{for } \mu = 2. \end{aligned} \quad (\text{A2})$$

2. $x(t) \in I^{(-)}$ for the time interval $t \in (t_0, T)$

Now $G(x) \leq 0$ (with the equality only at the borders of $I^{(-)}$) and

$$\frac{dx(t)}{dt} = d[-G(x)]^{\mu-1} D(x), \quad (\text{A3})$$

with $d = a + b\mu/2 \neq 0$ (again, the $d = 0$ case is trivial). Observe that $G_0 < 0$.

Finally, by integrating Eq. (A3) using Eq. (2) we get $(t \in (t_0, T))$

$$\begin{aligned} x(t) &= \tilde{G}(-[d(\mu-2)(t-t_0) + (-G_0)^{2-\mu}]^{1/(2-\mu)}), & \text{for } \mu \neq 2, \\ x(t) &= \tilde{G}(G_0 \exp[-d(t-t_0)]), & \text{for } \mu = 2. \end{aligned} \quad (\text{A4})$$

-
- [1] E. R. Nakamura, K. Kudo, O. Yamakawa, Y. Tamagawa (Eds.), Complexity and Diversity, Springer-Verlag, Tokyo, 1997.
- [2] S. E. Page, Diversity and Complexity, Princeton University Press, Princeton, 2011.
- [3] D. A. Rand, Measuring and characterizing spatial patterns, dynamics and chaos in spatially extended dynamical systems and ecologies, Philos. Trans. Phys. Sci. Eng. 348 (1688)(1994) 497-514.
- [4] D. A. Rand, H. B. Wilson, Using spatio-temporal chaos and intermediate-scale determinism to quantify spatially extended ecosystems, Proc. R. Soc. Lond. B 259 (1355) (1995) 111-117.
- [5] L. F. Cugliandolo, Coarsening phenomena, C. R. Phys. 16 (257) (2015) 257-266.
- [6] P. Mayer, H. Bissig, L. Berthier, L. Cipelletti, J. P. Garrahan, P. Sollich, V. Trappe, Heterogeneous dynamics of coarsening systems, Phys. Rev. Lett. 93 (11) (2004) 115701.
- [7] T. Stankovski, T. Pereira, P. V. E. McClintock, A. Stefanovska, Coupling functions: Universal insights into dynamical interaction mechanisms, Rev. Mod. Phys. 89 (4) (2017) 045001.
- [8] S. A. Agafonov, Stability of nonconservative systems and applications, J. Math. Sci. 125 (4) (2005) 556.

- [9] G. S. Cumming, *Spatial Resilience in Social-Ecological Systems*, Springer, Dordrecht, 2011.
- [10] N. V. Lowery, T. Ursell, Structured environments fundamentally alter dynamics and stability of ecological communities, *Proc. Nat. Acad. Sci.*, 116 (379) (2019) 379-388.
- [11] Y. Edri, E. Meron, A. Yochelis, Spatial heterogeneity may form an inverse camel shaped Arnol'd tongue in parametrically forced oscillations, *Chaos* 30 (2) (2020) 023120.
- [12] A. L. Krause, V. Klika, T. E. Woolley, E. A. Gaffney, Heterogeneity induces spatiotemporal oscillations in reaction-diffusion systems, *Phys. Rev. E* 97 (5) (2018) 052206.
- [13] Y. Edri, E. Meron, A. Yochelis, Spatial asymmetries of resonant oscillations in periodically forced heterogeneous media, *Physica D* 410 (2020) 132501 .
- [14] J.-W. Sun, Effects of dispersal and spatial heterogeneity on nonlocal logistic equations, *Nonlinearity* 34 (8) (2021) 5434.
- [15] M. Kimura, Diffusion models in population genetics, *J. Appl. Probability* 1 (177) (1964) 177-232.
- [16] Y. J. Liang, Q. Y. Allen, W. Chen, R. G. Gatto, L. Colon-Perez, T. H. Mareci, R. L. Magin, A fractal derivative model for the characterization of anomalous diffusion in magnetic resonance imaging, *Commun. Nonlinear Sci. Numer. Simul.* 39 (529) (2016) 529-537.
- [17] K. S. Fa, Fractal and generalized Fokker–Planck equations: description of the characterization of anomalous diffusion in magnetic resonance imaging, *J. Stat. Mech.* 2017 (3) (2017) 033207.
- [18] G. Aquino, M. Bologna, H. Calisto, An exact analytical solution for generalized growth models driven by a Markovian dichotomic noise, *Eurphys. Lett.* 89 (5) (2010) 50012.
- [19] P. J. Jackson, C. J. Lambert, R. Mannella, P. Martano, P. V. E. McClintock, N. G. Stocks, Relaxation near a noise-induced transition point, *Phys. Rev. A* 40 (5) (1989) 2875.
- [20] K. S. Fa, Langevin equation with multiplicative white noise: transformation of diffusion processes into the wiener process in different rescriptions, *Ann. Phys.* 327 (8) (2012) 1989-1997.
- [21] F. J. Richards, A flexible growth function for empirical use, *J. Exp. Bot.* 10 (2) (1959) 290-301.
- [22] S. Sakanoue, Extended logistic model for growth of single-species populations, *Ecol. Modelling* 205 (1) (2007) 159-168.
- [23] N. S. Goel, S. C. Maitra, E. W. Montroll, On the Volterra and other nonlinear models of interacting populations, *Rev. Mod. Phys.* 43 (2) (1971) 231.
- [24] P. R.-Román, F. T.-Ruiz, Modelling logistic growth by a new diffusion process: application to biological systems, *Biosys.* 110 (9) (2012) 9-21.

- [25] K. M. C. Tjørve, E. Tjørve, The use of Gompertz models in growth analyses, new Gompertz-model approach: An addition to the Unified-Richards family, *Plos One* 12 (6) (2017) e0178691.
- [26] P. N. Sen, Time-dependent diffusion coefficient as a probe of the permeability of the pore wall, *Chem. Phys.* 119 (18) (2003) 9871.
- [27] J. Wu, K. M. Berland, Propagators and time-dependent diffusion coefficients for anomalous diffusion, *Biophys. J.* 95 (4) (2008) 2049-2052.
- [28] L. Rubchinsky, M. Sushchik, Anomalous relationship between spatial and temporal patterns of dynamical behavior, *Internat. J. Bifur. Chaos* 9 (12) (1999) 2329-2333.
- [29] J. Bragard, S. Boccaletti, F. T. Arecchi, Control and synchronization of space extended dynamical systems, *Internat. J. Bifur. Chaos* 11 (11) (2001) 2715-2729.
- [30] G. Russo, J.-J. E. Slotine, Symmetries, stability, and control in nonlinear systems and networks, *Phys. Rev. E* 84 (4) (2011) 041929.
- [31] Z. G. Nicolaou, D. J. Case, E. B. van der Wee, M. M. Driscoll, A. E. Motter, Heterogeneity-stabilized homogeneous states in driven media, *Nature Commun.* 12 (1) (2021) 4486.
- [32] Y. Wang, X. Wang, D. Ren, Y. Ma, C. Wang, Effect of asymmetry on cooperation in spatial evolution, *Phys. Rev. E* 103 (3) (2021) 032414.
- [33] A. S. Pikovsky, M. G. Rosenblum, J. Kurths, *Synchronization: A Universal Concept in Nonlinear Sciences*, Cambridge University Press, Cambridge, 2001.
- [34] S. Boccaletti, J. Kurths, G. Osipov, D. L. Valladares, C. S. Zhou, The synchronization of chaotic systems, *Phys. Rep.* 366 (1) (2002) 1-101.
- [35] E. Mosekilde, Y. Maistrenko, D. Postnov, *Chaotic Synchronization: Applications to Living Systems*, World Scientific, Singapore, 2002.
- [36] S. H. Strogatz, *Sync: How Order Emerges From Chaos in The Universe, Nature, and Daily Life*, Hyperion, New York, 2004.
- [37] G. Barabás, C. Parent, A. Kraemer, F. V. de Perre, F. De Laender, The evolution of trait variance creates a tension between species diversity and functional diversity, *Nat. Commun.* 13 (1) (2022) 2521.
- [38] C. Manchein, R. M. da Silva, M. W. Beims, Proliferation of stability in phase and parameter spaces of nonlinear systems, *Chaos* 27 (2017) 081101.
- [39] R. M. da Silva, C. Manchein, M. W. Beims, Controlling intermediate dynamics in a family of quadratic maps, *Chaos* 27 (2017) 103101 (2017).

- [40] D. Dudkowski, S. Jafari, T. Kapitaniak, N. V. Kuznetsov, G. A. Leonov, A. Prasad, Hidden attractors in dynamical systems, *Phys. Rep.* 637 (2016) 1-50.
- [41] G. M. Zaslavsky, Dynamical traps, *Physica D* 168 (2002) 292-304.
- [42] S. C. Manrubia, A. S. Mikhailov, D. H. Zanette, *Emergence of Dynamical Order*, World Scientific, Singapore, 2004.
- [43] Y. B.-Yam, *Dynamics of Complex Systems*, Routledge, New York, 2019.
- [44] L. Arnonld, *Random Dynamical Systems*, Springer-Verlag, Berlin, 2002.
- [45] M. I. Freidlin, A. D. Wentzell, *Random Perturbations of Dynamical Systems*, Springer, Berlin, 2012.
- [46] J. V. S.-Filho, E. P. Raposo, A. M. S. Macêdo, G. L. Vasconcelos, G. M. Viswanathan, F. Bartumeus, M. G. E. da Luz, A Langevin dynamics approach to the distribution of animal move lengths, *J. Stat. Mec. The. Exp.* 2020 (2) (2020) 023406.
- [47] H. Risken, *The Fokker-Planck Equation*, Springer-Verlag, Berlin, 1996.
- [48] C.W. Gardiner, *Handbook of Stochastic Methods*, Springer-Verlag, Berlin, 1997.
- [49] W. T. Coffey, Y. P. Kalmykov, *The Langevin equation: With applications to stochastic problems in physics, chemistry, and electrical engineering*, New Jersey, World Scientific, 2017.
- [50] M. Gitterman, *The Noisy Oscillator*, World Scientific, Singapore, 2005
- [51] I. Snook, *The Langevin and Generalised Langevin Approach to the Dynamics of Atomic, Polymeric and Colloidal Systems*, Elsevier, Amsterdam, 2007.
- [52] K. S. Fa, *Langevin and Fokker-Planck equations and their generalizations*, World Scientific, Singapore, 2018.
- [53] C. Zoppou, J. H. Knight, Analytical solution of a spatially variable coefficient advection-diffusion equation in up to three dimensions, *App. Math. Modelling* 23 (9) (1999) 667-685.
- [54] Z. Ahmad, Numerical solution for advection-diffusion equation with spatially variable coefficients, *ISH J. Hydraulic Eng.* 6 (1) (2000) 46-54.
- [55] D. Rais, M. Mensik, B. Paruzel, P. Toman, J. Pflieger, Concept of the time-dependent diffusion coefficient of polarons in organic semiconductors and its determination from time-resolved spectroscopy, *J. Phys. Chem. C* 122 (40) (2018) 22876.
- [56] O. K. Dudko, A. M. Berezhkovskii, G. H. Weiss, Time-dependent diffusion coefficients in periodic porous materials, *J. Phys. Chem. B* 109 (45) (2005) 21296-21299.
- [57] L. F. Richardson, Atmospheric diffusion shown on a distance-neighbour graph, *Proc. R. Soc.*

- London, Ser. A 110 (756) (1926) 709-737.
- [58] A. N. Komolgorov, The local structure of turbulence in incompressible viscous fluid for very large Reynolds numbers, *Dokl. Acad. Sci. URSS* 30 (1941) 301-305.
- [59] G. K. Batchelor, Diffusion in a field of homogeneous turbulence: II. The relative motion of particles, *Proc. Cambridge Philos. Soc.* 48 (2) (1952) 345-362.
- [60] A. Okubo, A review of theoretical models for turbulent diffusion in the sea, *J. Oceanogr. Soc. Jpn.* 20 (1962) 286-320.
- [61] H. G. E. Hentschel and I. Procaccia, Relative diffusion in turbulent media: The fractal dimension of clouds, *Phys. Rev. A* 29 (3) (1984) 1461.
- [62] K. S. Fa, Exact solution of the Fokker-Planck equation for a broad class of diffusion coefficients, *Phys. Rev. E* 72 (2) (2011) 020101.
- [63] K. S. Fa, Solution of Fokker-Planck equation for a broad class of drift and diffusion coefficients, *Phys. Rev. E* 84 (2) (2011) 012102.
- [64] L. Schimansky-Geier, C. Zülicke, Harmonic noise: Effect on bistable systems, *Z. Phys. B* 79 (3) (1990) 451.
- [65] A. V. Barzykin, K. Seki, Stochastic resonance driven by Gaussian multiplicative noise, *Europhys. Lett.* 40 (2) (1997) 117.
- [66] K. G. Wang, M. Tokuyama, Nonequilibrium statistical description of anomalous diffusion, *Physica A* 265 (3) (1999) 341-351.
- [67] H. Calisto, M. Bologna, Exact probability distribution for the Bernoulli-Malthus-Verhulst model driven by a multiplicative colored noise, *Phys. Rev. E* 75 (5) (2007) 050103.
- [68] J. I. Jiménez-Aquino, M. Romero-Bastida, Mauricio. Non-Markovian stationary probability density for a harmonic oscillator in an electromagnetic field, *Phys. Rev. E* 86 (2012) (6) 061115.
- [69] K. S. Fa, A class of solvable nonlinear Langevin equation driven by multiplicative colored noise, *J. Stat. Mech.* 2019 (6) (2019) 063205.
- [70] K. S. Fa, A class of nonlinear Langevin equation with the drift and diffusion coefficients separable in time and space driven by different noises, *Physica A* 545 (2020) 123334.
- [71] K. S. Fa, Fokker-Planck equation with linear and time dependent load forces, *Eur. J. Phys.* 37 (6) (2016) 065101.
- [72] K. S. Fa, Similar solutions for nonlinear Langevin equations with the drift and diffusion coefficients separable in time and space, *J. Stat. Mech.* 2020 (9) (2020) 093206.

- [73] G. W. Bluman, J. D. Cole, *Similarity Methods for Differential Equations*, Springer-Verlag, Berlin, 1974.
- [74] W.-L. Lin, C.-L. Ho, Similarity solutions of the Fokker–Planck equation with time-dependent coefficients, *Ann. Phys.* 327 (2) (2012) 386-397.
- [75] C.-L. Ho, Similarity solutions of Fokker-Planck equation with moving boundaries, *J. Math. Phys.* 54 (4) (2013) 041501.
- [76] C.-L. Ho, R. Sasaki, Extensions of a class of similarity solutions of Fokker-Planck equation with time-dependent coefficients and fixed/moving boundaries, *J. Math. Phys.* 55 (11) (2014) 113301.
- [77] C.-L. Ho, C.-M. Yang, Convection-diffusion-reaction equation with similarity solutions, *Chin. J. Phys.* 59 (2019) 1117-125.
- [78] E. Agazzi, L. Montecucco (Eds.), *Complexity and Emergence*, World Scientific, Singapore, 2002.
- [79] S. Albeverio, E. Mastrogiacomo, E. R. Gianin, S. Ugolini (Eds.) *Complexity and Emergence*, Springer, Cham, 2022.
- [80] J. B. Avalos, I. Pagonabarraga, Phenomenological approach to nonlinear Langevin equations, *Phys. Rev. E* 52 (6) (1995) 5881.
- [81] A. Ryabov, V. Holubec, E. Berestneva, Living on the edge of instability, *J. Stat. Mec. Theor. Exp.* 2019 (8) (2019) 084014.
- [82] E. Mazumdar, T. Westenbroek, M. I. Jordan, S. S. Sastry, High confidence sets for trajectories of stochastic time-varying nonlinear systems, 2020 59th IEEE Conference on Decision and Control (CDC) (2020) 4275-4280
- [83] J. L. Callaham, J.-C. Loiseau, G. Rigas, L. S. Brunton, Nonlinear stochastic modelling with Langevin regression, *Proc. R. Soc. A* 477 (2250) (2021) 20210092.
- [84] K. Zhao, Stability of a nonlinear Langevin system of ML-type fractional derivative affected by bime-baryng delays and differential feedback control, *Fractal Fract.* 6 (12) (2022) 725.